PHOTONICS Research

Application of optical frequency division to radio frequency for simultaneous cancellation of the impact of laser and clock frequency noise on gravitational wave detection

Congyu Wang,[1] Haosen Shi,[1,4] Yuan Yao,[1,5] Hongfu Yu,[1] Longsheng Ma,[1,2] and Yanyi Jiang[1,2,3]

[1]State Key Laboratory of Precision Spectroscopy, East China Normal University, Shanghai 200062, China
[2]Collaborative Innovation Center of Extreme Optics, Shanxi University, Taiyuan 030006, China
[3]Hefei National Laboratory, Hefei 230088, China
[4]e-mail: hsshi@lps.ecnu.edu.cn
[5]e-mail: yyao@lps.ecnu.edu.cn

Received 8 May 2025; revised 16 July 2025; accepted 1 August 2025; posted 5 August 2025 (Doc. ID 567373); published 24 October 2025

To demonstrate the application of optical frequency division (OFD) in space-based gravitational wave (GW) detection, we conduct a ground-based test experiment utilizing optical interferometers and a purely optically divided radio frequency (RF) signal. The optically divided RF signal is generated using a microwave-referenced optical frequency comb. The comb frequency noise during OFD is suppressed by employing the transfer oscillator scheme, and the additional frequency instability in optical-to-10-MHz frequency division is 5×10^{-13} and 2×10^{-15} at 1 s and 1000 s, respectively. When this optical-to-10-MHz signal is used as the reference clock for frequency/phase measurement in GW detection, it can simultaneously reduce the impact of laser and clock frequency noise on GW detection, yielding a detection noise floor down to 10^{-6} Hz/Hz$^{1/2}$ at 1 mHz by utilizing the time-delay interferometer technique. This noise level meets the requirements of most space-based GW detectors. We also demonstrate that a division noise of no more than 10^{-11} is sufficient for comb-assisted GW detection.

https://doi.org/10.1364/PRJ.567373

1. INTRODUCTION

Gravitational wave (GW) detectors [1] typically employ laser interferometers and scientific lasers with extremely low frequency noise to detect weak GW signals. However, state-of-the-art ultrastable lasers alone are insufficient for space-based GW detectors. Unequal and time-varying interferometer arm lengths result in detection of uncancelled frequency noise from ultrastable lasers, which overwhelms the weak GW signals [2–4]. Moreover, owing to the relative velocities between spacecraft, the frequencies of the received laser light experience Doppler shifts. To compensate for these Doppler frequency shifts, ultrastable oscillators (USOs) at radio frequency (RF) are employed. Meanwhile, USOs are also used in laser phase locking and phase measurement. The noise from USOs is typically much higher than the weak GW signals. To mitigate the impact of frequency noise from both scientific lasers and USOs on GW detection, time-delay interferometry (TDI) is proposed. It is achieved by recording time-stamped data and interfering time-delayed data strings [5]. After such a post-processing procedure, the impact of frequency noise from lasers and USOs on GW detection is reduced to a level similar to that of ground-based laser interferometers with equal arm lengths.

In the TDI technique, a prerequisite for suppressing the impact of USO noise on GW detection is to calibrate the phase of all the USOs on different spacecraft, which necessitates phase modulation and phase measurement of laser beams exchanged between spacecraft [6]. An alternative approach relies on the use of an optical frequency comb (OFC) to generate an RF clock signal that is coherent to the scientific laser light [7]. With this clock, the modified second-generation TDI combinations (designated algorithms of observed laser interfering signals; see Ref. [7]) can simultaneously cancel both the impact of laser and clock frequency noises in GW detection. A test setup on the ground demonstrates that the impact of the laser frequency noise on GW detection can be suppressed by seven orders of magnitude [8]. However, in this test the down-converted RF signal is mixed with a hydrogen maser, rather than a purely optically divided RF clock. This mixed clock signal would underestimate the additional frequency noise in real GW detection since USOs on different spacecraft have uncorrelated noise that cannot be rejected. Later, an optically divided

RF clock is used to test the TDI technique, but the simulation of unequal-arm laser interferometers is realized with an electrical interferometer [9,10].

In this paper, we conduct a ground-based experiment to rigidly test the effectiveness of the comb-based TDI technique. Compared to previous works, we employ optical interferometers and a purely optically divided RF clock signal. The optically divided RF clock signal is generated by using a microwave-referenced OFC. With the technique of the transfer oscillator scheme [11], the additional frequency instability in optical-to-10-MHz frequency division is tested to be 5×10^{-13} and 2×10^{-15} at averaging times of 1 s and 1000 s, respectively, limited by the noise from direct digital synthesizers (DDSs). The results of the ground-based test experiment show that the impact of laser frequency noise on GW detection can be suppressed by seven orders of magnitude, down to 10^{-6} Hz/Hz$^{1/2}$ at a Fourier frequency of 1 mHz, which fulfills the requirements of most space-based GW detectors. We also demonstrate that when an RF clock uncorrelated to the optical signal is used, it will result in extra noise in GW detection. This measurement, on another side, shows the importance of using an RF clock correlated to the scientific laser. Moreover, we show that an additional frequency instability of no more than 10^{-11} in the optical-to-10-MHz division is sufficient for comb-based GW detection. Due to the inherent immunity to comb frequency noise in the optical-to-RF frequency division, our approach alleviates the need for highly precise OFCs, making it suitable for space-based applications.

2. OPTICAL-TO-RF FREQUENCY DIVISION BASED ON TRANSFER OSCILLATOR SCHEME

One scheme to realize optical-to-microwave frequency division involves detecting the repetition rate harmonics of an optically referenced frequency comb [12,13]. Despite yielding microwave signals with exceptionally low phase noise, this approach necessitates precise phase locking of the OFC to an optical reference. It imposes requirements on OFCs, i.e., low noise performance and high bandwidth actuators, and servos to achieve tight phase locking. Moreover, it is hard to maintain robust phase locking over a long time. Instead, OFCs can be robustly frequency-stabilized to an RF clock. However, such OFCs frequency-stabilized to an RF clock are generally noisier compared to optically referenced frequency combs. To mitigate the impact of comb frequency noise on optical-to-microwave frequency division, the transfer oscillator scheme can be adopted [14]. Recently, another kind of transfer oscillator scheme [15,16] was developed to generate ultralow phase noise microwave signals at tens of gigahertz using two DDSs and a highly linear photodiode. Despite the ultra-low phase noise, in practice the frequency of the generated microwave signal contains a residual comb repetition rate due to the limited frequency division bit number of DDSs, resulting in frequency deviation from the setting value by 1–10^3 Hz.

To improve the division accuracy, we employ another scheme [11]. We use an OFC to realize optical-to-RF frequency division. The frequency of a comb line is given by $\nu_N = N f_r \pm f_0$ with f_r the repetition rate, f_0 the carrier-envelope offset frequency, and N an integer number. As shown in Fig. 1(a), the beat notes between a 1064 nm continuous wave (c.w.) laser with a frequency of ν_L (also the scientific laser in the following GW detection test) and its two nearby comb teeth [N-th and $(N+1)$-th comb lines] are detected on the same detector, denoted as f_{b1} and f_{b1}^*. Both f_{b1} and f_{b1}^* are filtered and mixed on double balanced mixers with a detected signal of f_0. The mixer outputs, which are now free of f_0, are then frequency-divided by DDS1 and DDS2, respectively. Subsequently, the outputs of the two DDSs are mixed to generate an RF signal Δ. To totally remove the comb repetition rate f_r, the divisors of the DDSs are chosen to satisfy $N/(N+1) = k_1/k_2 = \mathrm{FTW}_2/\mathrm{FTW}_1$, where k_i and FTW_i $(i = 1, 2)$ are divisors and frequency tuning words (FTWs) of DDS_i, respectively. Even using DDSs with a 32-bit FTW, the divisors can be set to exactly satisfy the above equation. Thereby, the mixed RF signal of $\Delta = \nu_L(1/k_1 - 1/k_2)$ is only related to ν_L and is free of comb frequency noise. The frequency ratio between ν_L and the RF signal Δ is expressed as follows:

$$R_1 = \frac{\nu_L}{\Delta} = \frac{1}{\frac{1}{k_1} - \frac{1}{k_2}}. \tag{1}$$

We measure the additional frequency instability during OFD by comparing two signals of Δ divided from a single

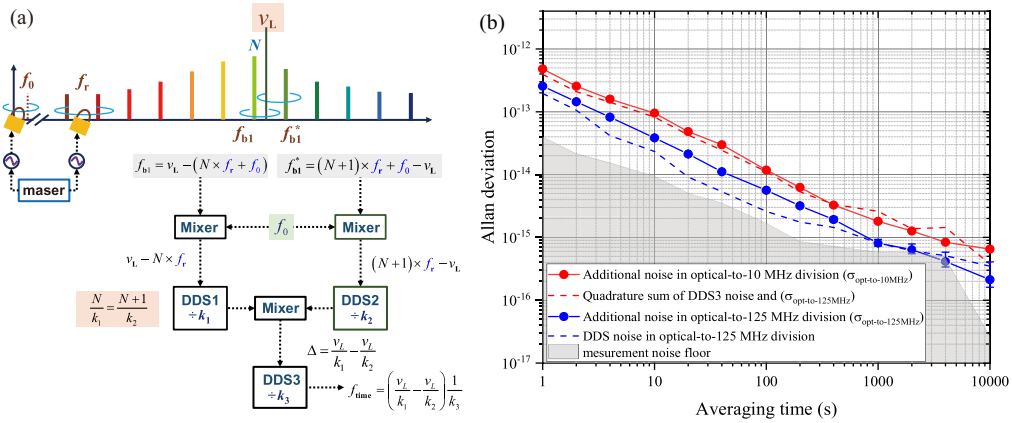

Fig. 1. (a) The experimental diagram of optical-to-RF frequency division based on transfer oscillator scheme. (b) Additional frequency instability during optical-to-RF frequency division when the frequency of the optically divided RF signal is 125 MHz and 10 MHz.

ν_L with two individual OFCs. The results are shown with blue dots in Fig. 1(b). When using two nearby comb teeth and Δ of around 125 MHz, the additional frequency instability in optical-to-125-MHz division is 2.6×10^{-13} and 8.1×10^{-16} at averaging times of 1 s and 1000 s, respectively. The gray area indicates the measurement noise floor. Meanwhile, the additional frequency noise from DDS1, DDS2, and the mixer used to generate the 125 MHz signal is plotted in a blue dashed line. As we can see from the figure, the additional frequency instability on short term during OFD is dominated by the noise of two DDSs. We find the noise of DDS trends down when its input frequency is increased. Therefore, by using beat notes against the $(N-1)$-th and $(N+2)$-th comb lines, which results in higher input frequencies for the DDSs, the contribution of DDS noise will reduce and thus a lower optical-to-RF frequency division noise is possible. Moreover, by adapting a multi-channel synchronized DDS array, the additional noise from DDS could be further suppressed [17]. Details of the method to estimate the measurement noise floor, DDS noise, and other contributions can be found in Appendix A.

In most cases, the acceptable frequency of the reference clock for RF synthesizers or frequency counters is 10 MHz. To meet this requirement, the generated RF signal of Δ at 125 MHz is then frequency-divided to nearly 10 MHz by DDS3 with a divisor of k_3. The resulting 10 MHz signal is expressed as $f_{\text{time}} = \nu_L/R$, where $R = R_1 \times k_3$. The additional frequency instability in the optical-to-10-MHz division is shown with red dots in Fig. 1(b), which is 4.8×10^{-13} and 1.8×10^{-15} at averaging times of 1 s and 1000 s, respectively. We also plot the estimated total noise in optical-to-10-MHz frequency division, including the measured noise of DDS3 and optical-to-125-MHz frequency division, as shown with a red dashed line. As the estimated total noise is close to the measured optical-to-10-MHz division noise, we attribute the degradation of noise in optical-to-10-MHz division to DDS3.

We also measure the uncertainty in optical-to-RF frequency division by comparing two RF signals divided from a single ν_L with two individual OFCs. The beat note between the two RF signals is measured with a frequency counter whose reference clock is f_{time}. The frequency ratio in optical-to-125-MHz division is measured to be deviated from the set value by $\delta R_1/R_1 \sim (3.5 \pm 4.2) \times 10^{-16}$, while that in optical-to-10-MHz division is deviated by $(1.1 \pm 2.4) \times 10^{-16}$. Both are limited by the statistical uncertainty.

Note that the scheme shown in Fig. 1 is based on an OFC coarsely stabilized to an RF frequency standard like a hydrogen maser or a rubidium (Rb) clock, which offers greater robustness compared to an optically referenced frequency comb. Furthermore, a single frequency comb can be used to generate multiple RF signals from different optical frequencies, making optical-to-RF frequency division more flexible and cost-efficient. Such accurate optical-to-RF frequency division is suitable for field and space applications.

3. TDI TECHNIQUE USING THE OPTICALLY DIVIDED RF SIGNAL

To demonstrate the feasibility of the comb-assisted TDI scheme in GW detection, we set up two Mach–Zehnder interferometers on the ground. Based on this setup, we tested the suppression of the impact of laser and clock frequency noise on GW detection using the TDI technique and the optically divided RF clock.

A space-based GW detector employs laser interferometers to measure GW-induced relative distance changes between three remote spacecraft. For simplicity, we use Fig. 2(a) to illustrate the space-based laser interferometer GW detector. Scientific laser light retroreflected from remoted spacecraft interferes with the local light on two photodetectors (PDs). Considering the Doppler frequency shift due to the movements of spacecraft, the beat notes detected on the i-th detector, $y_i(t)$, are expressed as

$$y_i(t) = \nu_L \times \frac{2V_i}{c} + \nu_{\text{noise}}(t - T_i) \times \left(1 - \frac{2V_i}{c}\right) - \nu_{\text{noise}}(t) + h_i(t), \tag{2}$$

where ν_L is the laser center frequency, $\nu_{\text{noise}}(t)$ the laser frequency noise at time t, V_i the relative velocity, T_i the delay time of the retroreflected light, c the speed of light, and $h_i(t)$ the gravitational signal. The first term of Eq. (2) represents the Doppler frequency shift due to the relative velocity between two spacecraft, denoted as $\Delta\nu_I = \nu_L \times 2V_i/c$, while the second and third terms represent uncommon laser frequency noise. Since $2V_i \ll c$, $\nu_{\text{noise}}(t - T_i)(1 - 2V_i/c) \approx \nu_{\text{noise}}(t - T_i)$. Thereby,

$$y_i(t) \approx \Delta v_i + v_{\text{noise}}(t - T_i) - v_{\text{noise}}(t) + h_i(t). \tag{3}$$

We set up two Mach–Zehnder interferometers on the ground, as shown in Fig. 2(b). The two interferometer arms are used to simulate the light paths exchanged between other spacecraft, heterodyne with a local arm on PD_1 and PD_2. The beat notes are denoted as $y_1(t)$ and $y_2(t)$. AOM_{2-5} are placed in each arm to shift the laser frequency differently in order to simulate Doppler frequency shifts and time-delayed laser frequency noise. Meanwhile, RF signals output from three synthesizers are used to drive AOM_{2-5} (AOM_2 and AOM_3 are driven by the same synthesizer), whose frequencies are controlled and programmed by a computer to simulate laser frequency noise and the time delay due to unbalanced arm lengths. The applied frequency noise is a white frequency noise. Figure 2(c) shows part of the added noise on the driving signals of AOM_{3-5}, which are delayed by T_1 and T_2. The driving signals are synthesized digitally from a hydrogen maser. The scientific laser is a cavity-stabilized laser at 1064 nm, which has a frequency instability of 6×10^{-16} at 1 s averaging time [18]. The laser light is separately sent to the laser interferometers and an OFC via optical fibers. The phase noise induced during transfer through optical fibers is actively cancelled [19]. In order to reduce amplitude modulation to phase modulation (AM-PM) noise, the light power is monitored on PD_0, and it is then actively stabilized by adjusting the driving power of AOM_1, resulting in a fractional light power instability of 3×10^{-4} at 10 s averaging time.

The optical-to-10-MHz signal is generated according to Section 2. Considering the laser frequency noise $\nu_{\text{noise}}(t)$, the generated RF signal can be expressed as

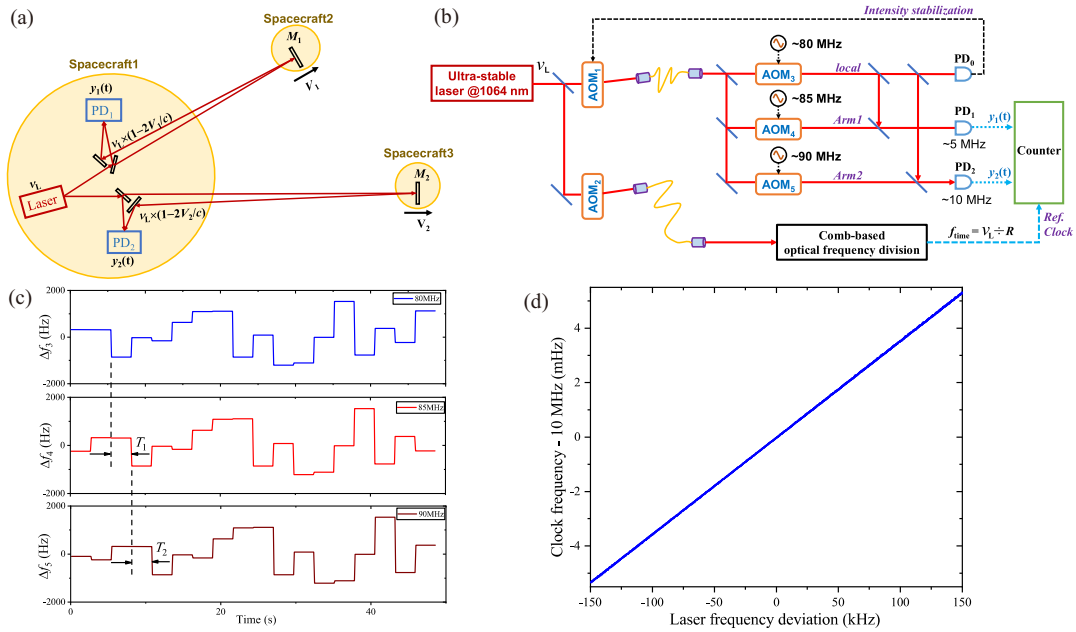

Fig. 2. (a) Simplified unequal three-arm Michelson interferometer for GW detection in space. PD, photodetector. AOM, acoustic-optical modulator. (b) Experimental setup for testing the validity of TDI with an optically divided RF clock. (c) Noise applied on AOMs. The center frequency of $f_{3\text{–}5}$ is 80 MHz, 85.05 MHz, and 90 MHz, respectively. The noises of AOM_4 and AOM_5 are delayed from that of AOM_3 by T_1 and T_2, respectively. (d) Optical-to-RF frequency division ratio measurement. The laser frequency is swept and measured against another laser. The optically divided RF clock frequency is measured against a stable RF reference.

$$f_{\text{time}}(t) = [\nu_{\text{L}} + \nu_{\text{noise}}(t)]/R = [\nu_{\text{L}} + \nu_{\text{noise}}(t)] \times \alpha = f_{t0} + \alpha\nu_{\text{noise}}(t), \tag{4}$$

where $\alpha = 1/R$, and $f_{t0} = \nu_{\text{L}}/R \approx 10$ MHz. This signal is used as the reference clock of a frequency counter to measure the beat notes detected on PD_1 and PD_2. As long as the divisors shown in Fig. 1(a) are set, the coefficient of α is fixed, even when we change the laser frequency. Figure 2(d) shows f_{time} when ν_{L} is changing. With this measurement, we determine $\alpha = 3.5506(2) \times 10^{-8}$, in accordance with the set values, which are determined by the divisors of the DDSs.

We denote the reading numbers of $y_i(t)$ on the frequency counter as

$$Y_i(t) = \frac{y_i(t)}{f_{\text{time}}(t)} \times 10^7 \text{ Hz} = \frac{y_i(t)}{f_{t0} + \alpha\nu_{\text{noise}}(t)} \times 10^7 \text{ Hz} \approx y_i(t)\left[1 - \frac{\alpha\nu_{\text{noise}}(t)}{f_{t0}}\right], \tag{5}$$

when the reference clock of the counter is $f_{\text{time}}(t)$. By substituting Eq. (3) into Eq. (5), and neglecting terms containing v_{noise}^2 and $\alpha h_i(t)$ [10^6 – 10^{13} times smaller than $h_i(t)$], we have

$$Y_i(t) = \Delta\nu_i + \nu_{\text{noise}}(t - T_i) - \nu_{\text{noise}}(t) - \alpha\left(\frac{\Delta\nu_i}{f_{t0}}\right)\nu_{\text{noise}}(t) + h_i(t). \tag{6}$$

Then, the second generation TDI combination $X(t)$, an algorithm designed to cancel out the laser frequency noise, can be calculated according to [7]

$$X(t) = \left[Y_1(t - T_2) - \left(1 + \alpha\frac{\Delta\nu_2}{f_{t0}}\right)Y_1(t)\right] - \left[Y_2(t - T_1) - \left(1 + \alpha\frac{\Delta\nu_1}{f_{t0}}\right)Y_2(t)\right]. \tag{7}$$

By substituting Eq. (6) into Eq. (7), and after neglecting the smaller terms containing $\alpha h_i(t)$, which is 10^8 times smaller than $h_i(t)$, we obtain the second generation TDI combination $X(t) \approx h_1(t - T_2) - h_1(t) - h_2(t - T_1) + h_2(t)$, which cancels the laser frequency noise but retains the GW signal.

We apply frequency noise with a standard deviation of 1 kHz to $AOM_{2\text{–}5}$. The delay times of AOM_4 and AOM_5 are set to be $T_1 = 3$ s and $T_2 = 6$ s, respectively. The blue and the red lines in Fig. 3 show the frequency noise of the signals detected on PD_1 and PD_2, which is 10–100 $\text{Hz}/\text{Hz}^{1/2}$ at a Fourier frequency of 1 mHz. When using the optically divided RF clock as the reference clock of the frequency counter and $\alpha = 3.5506 \times 10^{-8}$, we calculate the second-generation TDI combination $X(t)$ according to Eq. (7). By performing Fourier transformation, we obtain the frequency noise of $X(t)$ to be 10^{-6} $\text{Hz}/\text{Hz}^{1/2}$ at 1 mHz, as shown with the black line in Fig. 3. It is seven orders of magnitude smaller than the laser frequency noise. This result is close to the LISA requirement (yellow line) [7,8] and the measurement noise floor (green line).

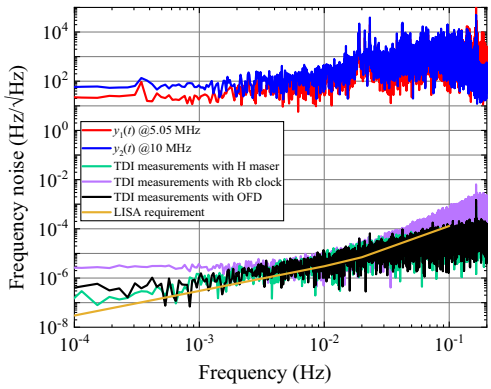

Fig. 3. TDI experimental results using an optically divided RF clock (black line), the same H maser (green line), and an independent rubidium clock (purple line) as the reference clock of the frequency counter. The frequency noises detected on PD1 and PD2 are also shown with a red line and a blue line, respectively.

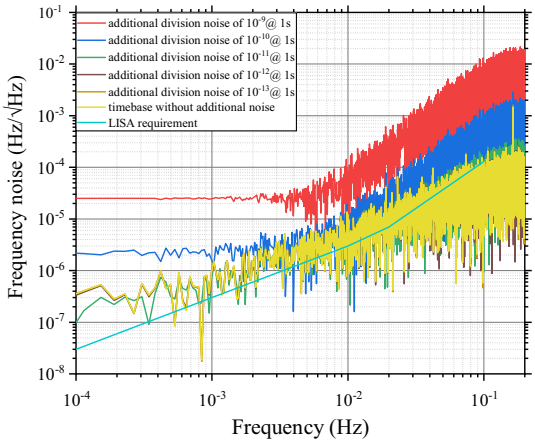

Fig. 4. TDI simulation results when using an optically divided RF clock together with artificially added division noise.

The measurement noise floor is the measured $X(t)$ when the reference clock of the frequency counter is from the maser and $\alpha = 0$. In this case, since the frequency noise applied to AOM_{3-5} is also synthesized from the maser, the frequency noise from the maser is common and cancelled, indicating that the measurement noise floor is independent of any RF clocks. Currently, the noise floor in the mHz frequency range is limited by the long-term optical length change of the interferometers induced by the temperature fluctuation of AOMs and the optical board. We also show the frequency noise of $X(t)$ when the reference clock of the counter is a Rb clock, while the noise applied to AOM_{3-5} is synthesized from the maser, as shown with the purple line in Fig. 3. Since the Rb clock and the maser are independent, their frequency noise cannot be totally cancelled via the second-generation TDI combination. This demonstrates the significance of clock synchronization between different spacecraft, which motivates clock phase noise cancellation between spacecraft or the use of the optically divided RF clock [7].

4. DISCUSSION

Benefiting from the immunity to comb frequency noise due to the transfer oscillator scheme, it places less demand on combs. Even when using a loosely frequency-stabilized comb or a free-running comb to realize optical-to-RF frequency division, we can suppress the impact of both the frequency noise of the laser and clock on GW detection down to 10^{-6} Hz/Hz$^{1/2}$ at 1 mHz. This makes comb-based TDI possible in space-based GW detection.

We also investigate the effect of noise in optical-to-microwave frequency division on the aforementioned comb-based TDI experiment. We numerically simulate the frequency noise of $X(t)$ when adding a white frequency noise onto the reading values of the counter, which simulates the additional noise added in optical-to-10-MHz frequency division. As shown in Fig. 4, the frequency noise of $X(t)$ after applying the TDI technique can be clearly observed when the division noise exceeds 10^{-11} at 1 s averaging time. This places fewer requirements on optical-to-RF frequency division in real space borne applications.

5. CONCLUSION

In summary, we show that the additional frequency instability induced in the optical-to-10-MHz frequency division using a microwave referenced optical comb is 5×10^{-13} and 2×10^{-15} at averaging times of 1 s and 1000 s, respectively, and it is not limited by the comb frequency noise. By employing the optically divided RF signal as a reference clock in space-based GW detection, we demonstrate that by using the TDI technique, the impact of laser frequency noise on GW detection can be suppressed by seven orders of magnitude, down to below 10^{-6} Hz/Hz$^{1/2}$ at 1 mHz. Moreover, the impact of the clock frequency noise on GW detection can be simultaneously cancelled in a single step. With simulations, we show that an additional frequency instability of no more than 10^{-11} in the optical-to-10-MHz frequency division is sufficient for GW detection. It reduces the strain on onboard USOs by using the optically divided RF signal as the reference clock, and it also eliminates the need for associated clock calibration systems. Such a scheme is feasible in space-based applications due to its lower demand on OFCs.

APPENDIX A

1. Experimental Parameters in Generating the Optically Divided RF Signal

In our experiment $\nu_L = 281.63951$ THz, $f_r = 999.581815$ MHz, and corresponding comb mode $N = 281,757$. When the FTWs of DDS1 and DDS2 are set to 536,748,990 and 536,747,085, respectively, the condition $N/(N+1) = k_1/k_2 = \mathrm{FTW}_2/\mathrm{FTW}_1$ is met. As a result, the generated RF clock signal is purely referenced to the optical frequency with an accurate frequency ratio.

2. Frequency Measurement Noise Floor

The measurement noise floor is measured by counting the frequency difference (~200 kHz) between two RF signals at approximately 125 MHz synthesized from a hydrogen maser

using two RF synthesizers. The reference clock of the frequency counter is from the same maser. The measurement result includes not only the measurement noise of frequency counters (K + K, FXE system) but also that from RF synthesizers (R&S, SMB100A) and the mixer. As a result, it gives an upper limit for the frequency measurement noise floor, as shown with the gray area in Fig. 1(b).

3. Measurement of DDS Noise

The RF output of a signal generator is power split and sent to two independent DDSs. The divisors of the two DDSs are set to make the frequency difference of the DDS outputs be 100–200 kHz for frequency counting with enough resolution. The signal generator and the frequency counter are both referenced to the same hydrogen maser. Since the DDSs share the same signal input, and both the signal generator and the frequency counter share the same reference clock, the measured frequency fluctuations of the beating signal directly reflect the intrinsic division noise of the DDSs, as the common noise is mostly rejected.

The noise of DDS trends down when the input frequency gets higher. Noise measurement of DDSs shows when a DDS divides a signal at ∼200 MHz to 50 MHz, the division noise of the DDS is about 2×10^{-13} at 1 s averaging time. When a DDS divides a signal at ∼800 MHz to 200 MHz, the division noise will be reduced to $\sim 5 \times 10^{-14}$ at 1 s averaging time.

In the main text, the DDS noise contribution to the optical-to-125-MHz division is estimated from the measured noise of DDS1 and DDS2 in Fig. 1(a). The input frequencies for DDSs during noise measurement are kept the same as those used in the optical-to-125-MHz frequency division. Considering the noises of two DDSs at two working frequencies are uncorrelated, we quadrature-sum their noise as the total noise contribution of DDSs in the optical-to-125-MHz frequency division.

4. Estimation of Photodetection Noise in Optical-to-RF Frequency Division

Photodetectors are also noise contributors in optical-to-RF frequency division as the amplitude noise of laser light will convert to phase noise due to the amplitude-to-phase conversion. In our case, it mainly comes from the photodetector detecting the beat note between the c.w. laser and its nearby comb teeth, f_{beat}. To estimate its noise, we lock two combs to the same optical reference. Then, two f_{r} signals of two combs are detected with the photodetectors used to detect f_{beat}. The relative frequency fluctuation between two f_{r} signals is recorded, which shows a frequency instability of 8.5×10^{-14} at 1 s averaging time. It includes the frequency noise from the photodetectors, measurement setups, servos, optical path fluctuation, etc. Therefore, this noise is the upper noise limit of the photodetectors. As the noise of photodetectors is small compared to that contributed from DDSs, we conclude it is not the major bottleneck for the current setup.

Funding. National Natural Science Foundation of China (12334020, 12341404, 12404552, 11927810); National Key Research and Development Program of China (2022YFB3904001); Innovation Program for Quantum Science and Technology (2021ZD0300904); Zhangjiang Laboratory (ZJSP21A001).

Acknowledgment. We thank Albrecht Bartels for prompt technical support on the turnkey Ti:sapphire mode-locked laser.

Disclosures. The authors declare no conflicts of interest.

Data Availability. Data underlying the results presented in this paper are not publicly available at this time but may be obtained from the authors upon reasonable request.

REFERENCES

1. B. P. Abbott, R. Abbott, T. D. Abbott, *et al.*, "Observation of gravitational waves from a binary black hole merger," Phys. Rev. Lett. **116**, 061102 (2016).
2. K. Danzmann, T. A. Prince, P. Binetruy, *et al.*, "LISA: unveiling a hidden universe," ESA/SRE (2011).
3. Y. Gong, J. Luo, and B. Wang, "Concepts and status of Chinese space gravitational wave detection projects," Nat. Astron. **5**, 881–889 (2021).
4. W.-R. Hu and Y. L. Wu, "The Taiji Program in Space for gravitational wave physics and the nature of gravity," Natl. Sci. Rev. **4**, 685–686 (2017).
5. M. Tinto and S. V. Dhurandhar, "Time-delay interferometry," Living Rev. Relativ. **17**, 6 (2014).
6. M. Tinto, F. B. Estabrook, and J. W. Armstrong, "Time-delay interferometry for LISA," Phys. Rev. D **65**, 082003 (2002).
7. M. Tinto and N. Yu, "Time-delay interferometry with optical frequency comb," Phys. Rev. D **92**, 042002 (2015).
8. Q. Vinckier, M. Tinto, I. Grudinin, *et al.*, "Experimental demonstration of time-delay interferometry with optical frequency comb," Phys. Rev. D **102**, 062002 (2020).
9. H. Wu, P. Wang, P. Hao, *et al.*, "Time delay interferometry using laser frequency comb as the direct signal source," Opt. Lasers Eng. **151**, 106938 (2022).
10. H. Wu, M. Xu, P. Wang, *et al.*, "Time delay interferometry with a transfer oscillator," Opt. Lett. **48**, 9–12 (2023).
11. Y. Yao, Y. Jiang, H. Yu, *et al.*, "Optical frequency divider with division uncertainty at the 10^{-21} level," Natl. Sci. Rev. **3**, 463–469 (2016).
12. T. M. Fortier, M. S. Kirchner, F. Quinlan, *et al.*, "Generation of ultrastable microwaves via optical frequency division," Nat. Photonics **5**, 425–429 (2011).
13. T. M. Fortier, A. Rolland, F. Quinlan, *et al.*, "Optically referenced broadband electronic synthesizer with 15 digits of resolution," Laser Photonics Rev. **10**, 780–790 (2016).
14. H. R. Telle, B. Lipphardt, and J. Stenger, "Kerr-lens, mode-locked lasers as transfer oscillators for optical frequency measurements," Appl. Phys. B **74**, 1–6 (2002).
15. P. Brochard, S. Schilt, and T. Südmeyer, "Ultra-low noise microwave generation with a free-running optical frequency comb transfer oscillator," Opt. Lett. **43**, 4651–4654 (2018).
16. N. V. Nardelli, T. M. Fortier, M. Pomponio, *et al.*, "10 GHz generation with ultra-low phase noise via the transfer oscillator technique," APL Photonics **7**, 026105 (2022).
17. M. Pomponio, A. Hati, and C. Nelson, "Ultra-low phase noise frequency division with array of direct digital synthesizers," IEEE Trans. Instrum. Meas. **73**, 5501310 (2024).
18. C. Yan, H. Shi, Y. Yao, *et al.*, "Long-term frequency-stabilized lasers with sub-hertz linewidth and 10^{-16} frequency instability," Chin. Opt. Lett. **20**, 070201 (2022).
19. L. S. Ma, P. Jungner, J. Ye, *et al.*, "Delivering the same optical frequency at two places: accurate cancellation of phase noise introduced by an optical fiber or other time-varying path," Opt. Lett. **19**, 1777–1779 (1994).